EasyChair Preprint

№ 5759

A Study on Application of Strain Indices for Seismic Performance Verification to Real-Scale RC Member by 3D Nonlinear FEA

Satoshi Komatsu, Yoshinori Miyagawa and Toyofumi Matsuo

June 7, 2021

A Study on Application of Strain Indices for Seismic Performance Verification to Real-Scale RC Member by 3D Material Nonlinear FEA

Satoshi Komatsu[1], Yoshinori Miyagawa[2,*], Toyofumi Matsuo[3]

1. Ph.D., Research Scientist, Structural Engineering Sector, Civil Engineering Research Laboratory, Central Research Institute of Electric Power Industry, Chiba, Japan
2. Ph.D., Senior Research Scientist, External Natural Event Research Team, Nuclear Risk Research Center, Central Research Institute of Electric Power Industry, Chiba, Japan
3. Ph.D., Senior Research Scientist, Structural Engineering Sector, Civil Engineering Research Laboratory, Central Research Institute of Electric Power Industry, Chiba, Japan

[*]Corresponding author email: komatsu3762@criepi.denken.or.jp

Abstract

In this research, the applicability of seismic performance verification indices based on the strain index calculated by three-dimensional material nonlinear finite element analysis was verified for real-scale RC members subjected to bilateral loadings. The verification was conducted by using three strain indices: main tensile strain (ε_t), main compressive strain ($|\varepsilon_c|$), and main shear strain ($|\varepsilon_{sh}|$). The average strain in the elements was used for each index. In addition, the second strain invariant of deviatoric strain tensor ($\sqrt{J'_2}$) and consumed strain energy (W_n), which are assumed to be less affected by element size, were also examined. The areas verified were two patterns: all the members and the core concrete.

As a result, it was found that all the indices reached the limit state before the maximum load capacity because they reached the limit value in cover concrete when all the elements were set as the area to be verified. In other words, it is possible to make a rational evaluation linked to a physical phenomenon, which is a reduction of shear load capacity due to the fracture of the core concrete, when the verification is conducted only in core concrete. It was also confirmed that $\sqrt{J'_2}$ and W_n were conservatively evaluated compared with other strain indices. The three strain indices (ε_t, $|\varepsilon_c|$, $|\varepsilon_{sh}|$), which are easily affected by element size, could be reasonably evaluated within this study. The reason is that large-scale members naturally have large element dimensions, making it difficult for large strain to be generated locally. Furthermore, it was clarified that all verification indices reached the limit values while maintaining sufficient load capacity in all the RC members with post-installed shear reinforcement, horizontal two-directional loadings, or initial damage (cracks) in the orthogonal direction.

Keywords: *3D material nonlinear FEA, seismic performance verification indices, real-scale RC member, horizontal two-directional loadings.*

1. Current structural performance verification method for underground RC box culvert in nuclear power plant by material non-linear FEM

The authors are working on the refinement and standardization of seismic performance verification methods for RC underground structures (Fig. 1) that compose emergency cooling facilities for nuclear power plants. Seismic performance verification of RC underground box culverts is based on two-dimensional analysis because the cross-sectional direction, which generally has a relatively small shear modulus with respect to horizontal force during an earthquake, is the target. On the other hand, it is effective to select three-dimensional analysis when the seismic response in the cross-sectional direction of the structure is not dominant or when the response behaviour of the structure is strictly evaluated.

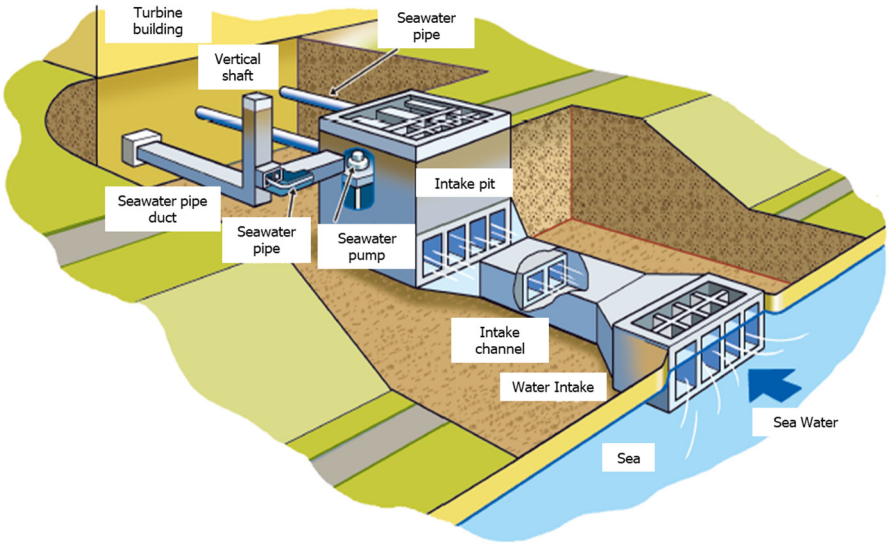

Figure 1. An example of underground reinforced concrete structures in nuclear power stations.

Therefore, the authors conducted a loading experiment on full-scale RC members repeatedly subjected to horizontal bidirectional force until shear fracture or bending fracture. Furthermore, the behaviours of the numerical analysis models created by the three-dimensional material nonlinear finite element method (FEM) were investigated during the loading process, and the applicability of the analysis models was confirmed and verified.

In this paper, based on the results of behaviour analysis, we investigated the applicability of seismic performance verification indices using strain-based indices calculated by the three-dimensional material nonlinear finite element method analysis. These indicators have been shown to be useful in past reports such as JSCE (Japan Society of Civil Engineers) specifications. However, this was a study under limited conditions, and verification is limited, especially for full-scale structural members. These indices were selected because they ought to be considered in view of their importance in practice.

2. Outline of experiment

2.1. Overview of specimens

The types of specimens are shown in Table 1. There are four types of test bodies in all, and one test body was cast for each test case. There are 4 patterns of test cases, and one specimen was made for each test case. In the basic case (N-1), the specimen was designed to show diagonal tensile failure. The shear strength is 1135.0 kN and the bending shear strength ratio is 0.85. Figure 2 shows the dimensions of the specimen with post-construction shear reinforcing bars (P-1) and the positions of the strain gauges. The structural specifications of the specimens (N-1, N-2-1, N-2-2) other than P-1 are the same except for the post-installed shear reinforcing rebars. The post-installed shear reinforcing rebars were constructed from one side, considering that the back of the site is the ground. The ratio of the main reinforcing bars in the columns is 1.58%.

Table 1. Specimen series.

Case Name	Points of Interest	Shear Reinforcement Rebar Ratio	Failure Mode
N-1	Base	0.08%	Diagonal tensile
P-1	Post-installed shear reinforcement	0.08+0.36% (post-installed)	Bending compression
N-2-1	Diagonal loading	0.08%	Diagonal tensile
N-2-2	Initial damage	0.08%	Diagonal tensile

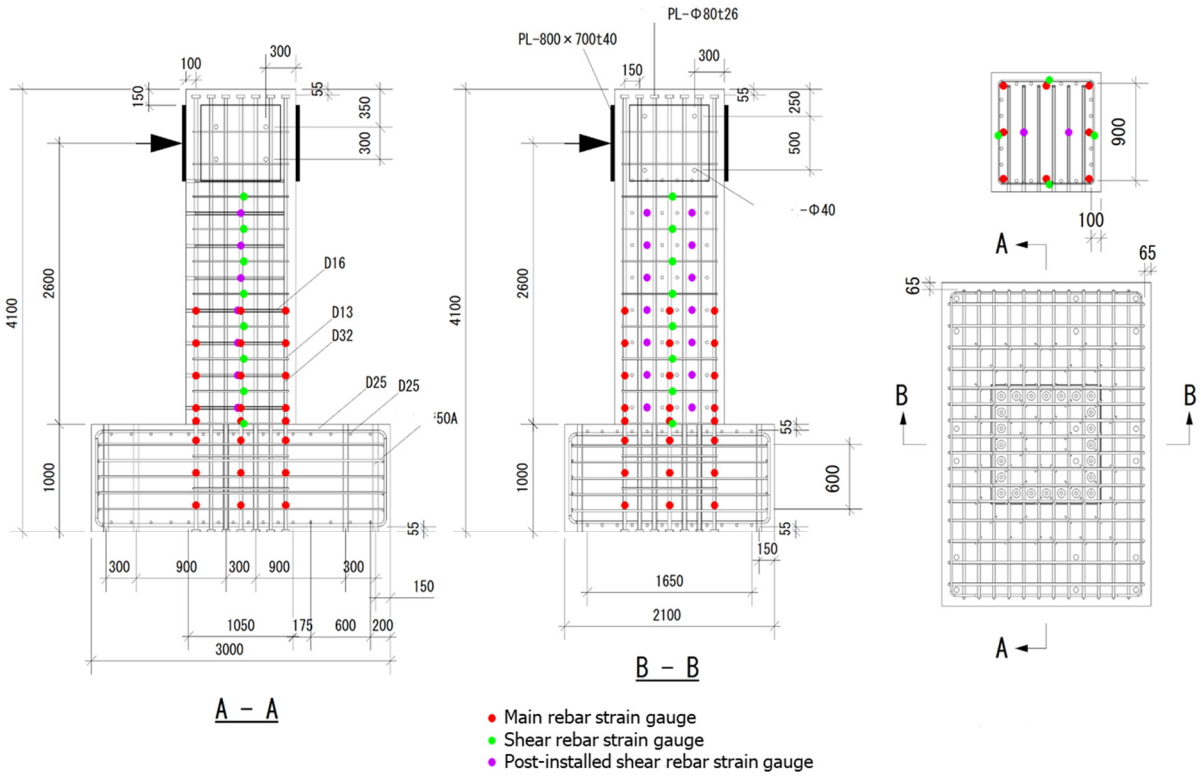

Figure 2. Specimen overview (P-1).

2.2. Materials used

Table 2 shows the mix composition of concrete for the specimens. The compressive strength and the Young's modulus were determined on the loading date. Table 3 shows the physical characteristics of concrete. The tensile strength was calculated by the equation from the JSCE specifications. Table 4 shows the physical characteristics of the reinforcing rebars.

Table 2. Mix proportion of concrete.

G_{max} (mm)	Slump (cm)	Air Content (%)	W/C (%)	s/a (%)	Unit Weight (kg/m^3)						
					C	W	S	G_1	G_2	G_3	Ad
20	12±2.5	4.5±1.5	59.6	49.1	272	162	909	382	283	292	2.72

Table 3. Physical characteristics of concrete.

Case Name	f_c [N/mm^2]	E_c [kN/mm^2]	f_t [N/mm^2]
N-1	36.9	30.0	2.5
P-1	36.2	29.9	2.5
N-2-1	39.1	30.8	2.6
N-2-2	39.0	30.7	2.6

Table 4. Physical characteristics of steel rebars.

	f_y [N/mm^2]	f_t [N/mm^2]	E_s [kN/mm^2]
Main rebar (D32)	508	676	196
Shear rebar (D13)	360	476	188
Post-installed shear rebar (D16)	396	584	188

2.3. Loading procedure

The loading axis name and loading pattern are shown in Figure 3. By pushing and/or pulling two jacks (at the same time), it is possible to apply loads in various directions to the specimen in two horizontal directions. The "□" in the column of the loading image diagram is an image of the pillar viewed from directly above (loading direction 1 from bottom to top and loading direction 2 from left to right).

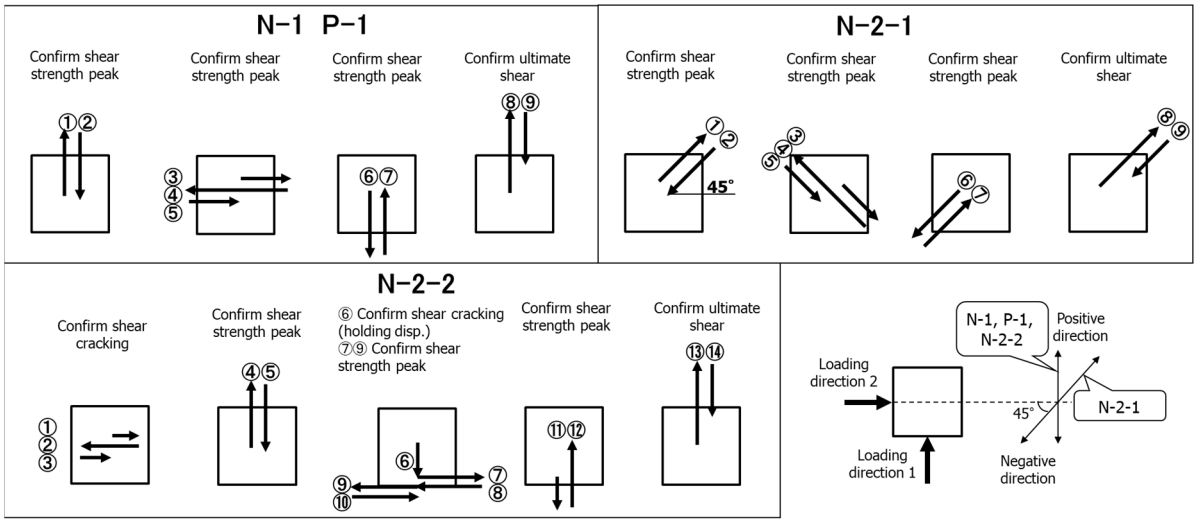

Figure 3. Loading patterns.

3. Analysis conditions

3.1. Analysis method

In this study, a three-dimensional material nonlinear finite element method analysis program, COM3, was used. This is a three-dimensional extension of the RC plane model based on the material nonlinear configuration model, which considers the arbitrary loading history. This analysis program shows high analysis accuracy in the past studies. The average strain-stress relationship of concrete consists of one-dimensional compression, tension, and shear transfer models on cracked surfaces, each of which is time-dependent. By using the multi-directional non-orthogonal fixed crack model, it is possible to reproduce the occurrence and post-occurrence of multiple multi-directional cracks that occur according to the loading history.

In the constitutive law of the RC element, the strain hardening (restraint effect) of concrete by reinforcing bar can be considered before the occurrence of cracks by dividing the elements in consideration of the actual density and directionality of reinforcing bars. After a crack occurs, the tensile hardening model has been considered for RC elements, considering the effect of bonding between the reinforcing bar and concrete on a spatial average. On the other hand, the tensile softening model obtained from fracture energy and element dimensions is being considered for plane concrete elements.

3.2. Element divisions

Figure 4 shows an overview of element divisions. In order to properly consider the bonding effect between the reinforcing bar and concrete, the cross section of the column was divided into RC element and plane concrete element as shown in the figure, considering the position of the main reinforcing bars, referring to previous studies. Shear reinforcing bars were treated as being uniformly dispersed in the columns, for a constant reinforcing bar ratio in the columns.

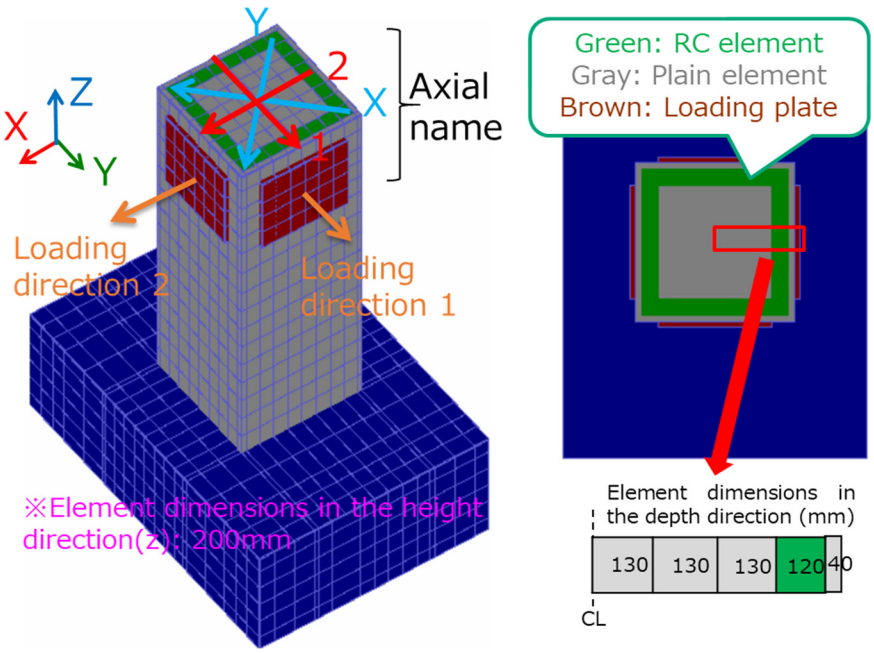

Figure 4. Element division.

3.3. Input data

Basically, the results of the material test were used as shown in Tables 3 and 4. Regarding the tensile strength of concrete, the tensile strength calculated by the value of compressive strength following the JSCE specifications was reduced to about 60% considering the shrinkage stress generated on the concrete surface due to drying shrinkage. The tensile hardening coefficient of the RC element and the tensile softening coefficient of the plane concrete element were set as shown in Table 5, referring to past studies. In the experiment, immediately after confirming the maximum proof stress, the load capacity decreased because the horizontal displacement was maintained for observing cracks. Since time dependence is taken into consideration in this analysis program, it was decided to hold the horizontal displacement, for which the maximum load capacity was confirmed, uniform for 30 minutes.

Table 5. Tension softening / stiffening coefficient.

RC Element			Plan Element
Main rebar direction	Shear reinforcement rebar direction	Orthogonal direction of rebar	
0.4	0.8	2.0	4.0

4. Verification index

In Japan, the performance verification method using nonlinear FEM was adopted in the 2012 JSCE specifications. In these specifications, not only the accuracy of the response value was improved, but the limit value with high versatility was examined. In this study, the deviation strain second invariant ($\sqrt{J'_2}$) and the normalized cumulative strain energy W_n, which were spatially weighted averaged, were used as indices. The average length was set to 150 mm, and the limit value examples were set to 1000 μ and 1500 μ, respectively. The former corresponds to crack damage and the latter corresponds to compression damage.

Deviation strain second invariant:

$$\sqrt{J_2'} = \sqrt{\frac{2}{3}\left\{\left(\frac{\varepsilon_x-\varepsilon_y}{2}\right)^2+\left(\frac{\varepsilon_y-\varepsilon_z}{2}\right)^2+\left(\frac{\varepsilon_z-\varepsilon_x}{2}\right)^2\right\}+\left(\frac{\gamma_{xy}}{2}\right)^2+\left(\frac{\gamma_{yz}}{2}\right)^2+\left(\frac{\gamma_{zx}}{2}\right)^2} \quad (1)$$

Normalized cumulative strain energy:

$$W_n = \frac{1}{f}\sum_{k=1}^{n}\left(\sigma_x \cdot d\varepsilon_x + \sigma_y \cdot d\varepsilon_y + \sigma_z \cdot d\varepsilon_z + \tau_{xy} \cdot d\gamma_{xy} + \tau_{yz} \cdot d\gamma_{yz} + \tau_{zx} \cdot d\gamma_{zx}\right)^{(k)} \quad (2)$$

On the other hand, the main tensile strain (ε_t), main compressive strain ($|\ \varepsilon_c\ |$), and maximum shear strain ($|\ \varepsilon_{sh}\ |$) were also applied as damage indices corresponding to various damage modes of concrete materials. Based on the evaluation results in the previous reports, these values were set to 30,000 μ (3%), 10,000 μ (1%), and 20,000 μ (2%), respectively. These indices are not averaged considering element size dependence.

As the verification area of the above all indices, two cases were examined when the evaluation indices were applied to all the elements of the specimen and when it was applied to the plane concrete element arranged inside the main reinforcing bars.

5. Summary of behaviour analysis results

5.1. Load-displacement relationship

Figure 5 shows the load-displacement relationship of each specimen, N-1, P-1, N-2-1, and N-2-2, respectively. The solid line shows the analysis value, and the dotted line shows the experimental value. The numbers represent the loading order. In all four loading patterns and all loading processes, the difference in maximum load capacity between the experimental value and the analysed value was 30% or less at the maximum. In the JSCE specifications, γ_b = 1.3 is specified as the member coefficient of the shear loading capacity evaluation formula borne by concrete. This value takes into account the fact that shear fracture is an undesirable mode of fracture and that shear fracture is affected by boundary conditions and is susceptible to experimental variation. It was confirmed that the analysis method applied in this study is within this range as a guideline for the analysis accuracy related to shear loading capacity.

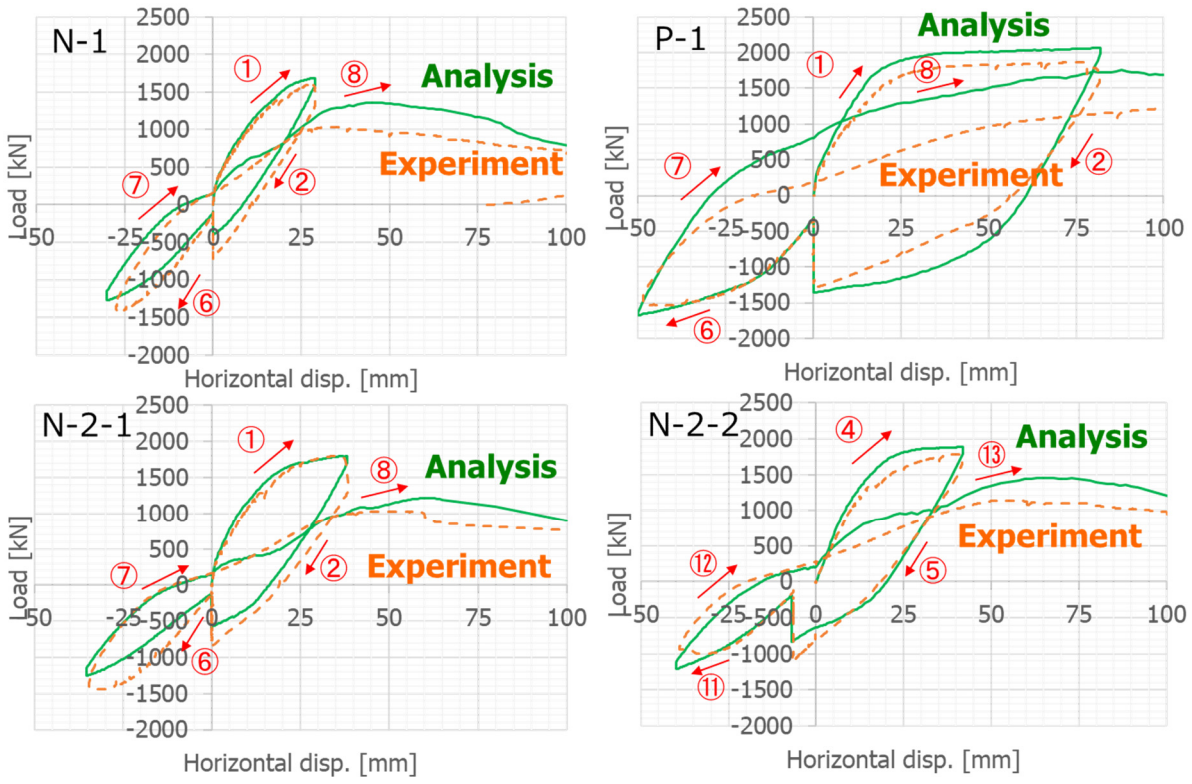

Figure 5. Load-disp. relationships.

5.2. State of destruction

Figure 6 indicates the principle strain contour diagram and crack condition of each specimen, N-1, P-1, N-2-1, and N-2-2, respectively. It was confirmed that the destructive situations were also qualitative, but roughly consistent.

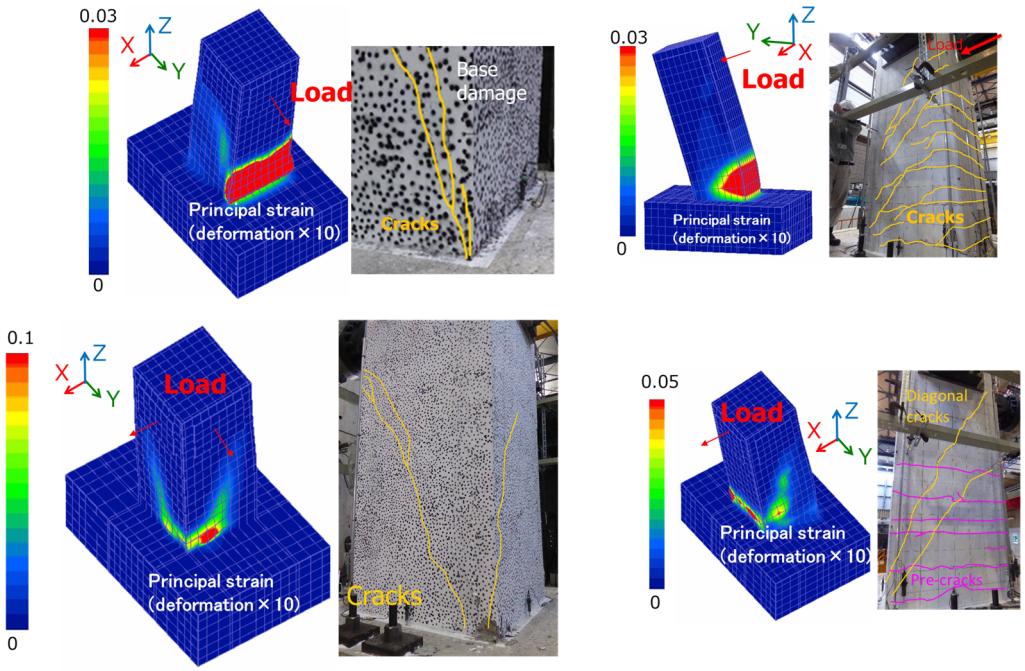

Figure 6. Failure mode of each specimen.

6. Examination results of verification indices

6.1. In case all elements are subject to verification

Figure 7 shows the load-displacement relationship of each specimen, N-1, P-1, N-2-1, and N-2-2, respectively. The value of each index (calculated by extraction from the analysis result) and load capacity calculated from the JSCE specifications are also shown in the figure. The numbers represent the loading order. It was found that $\sqrt{J'_2}$ and W_n were evaluated as marginal states at a stage where the load level is relatively low, regardless of the type of specimen. On the other hand, each strain index of main tensile strain (ε_t), main compressive strain ($|\varepsilon_c|$), and maximum shear strain ($|\varepsilon_{sh}|$) showed a limit state at about the maximum loading capacity.

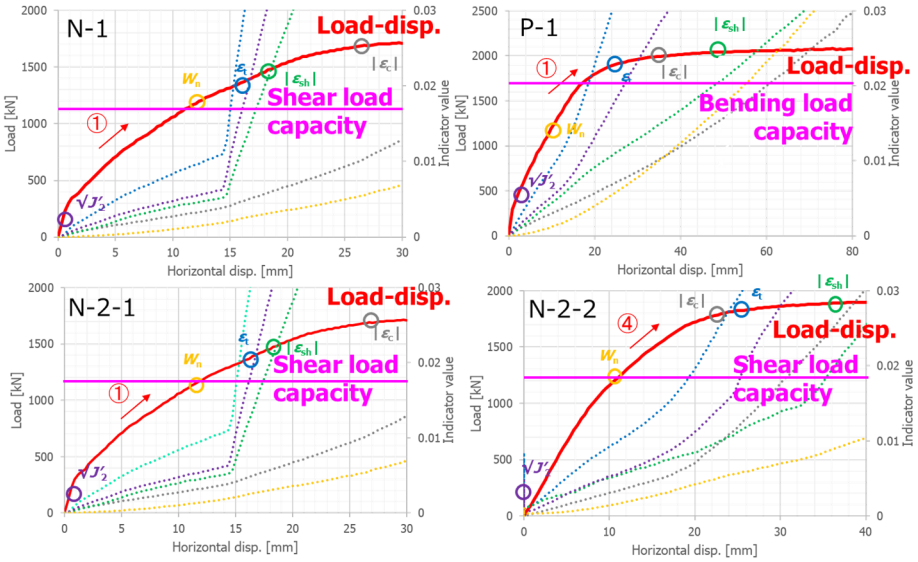

Figure 7. Load-disp. relationships and indicator values.

Figure 8 shows the positions determined to be in the limit state for each specimen. All indices reached the limit at the position of the element of the cover concrete.

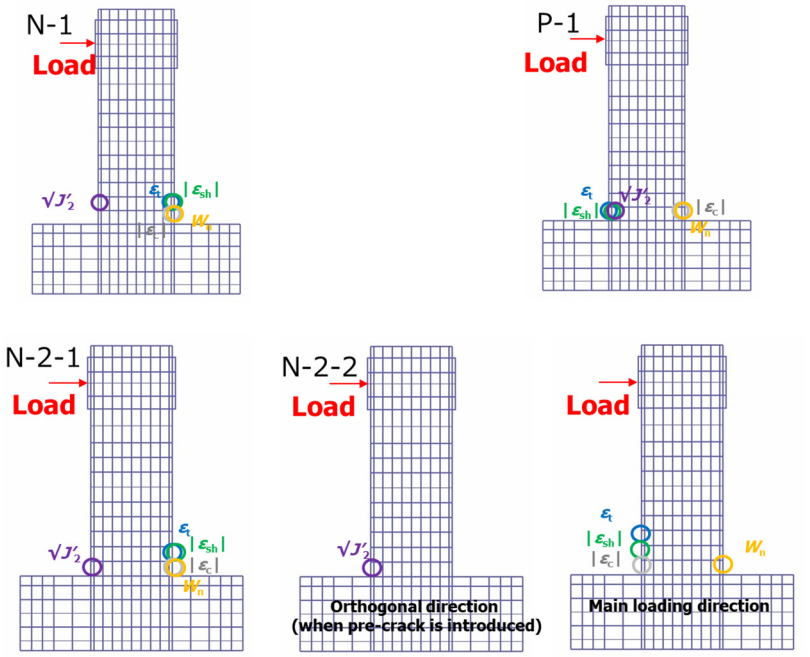

Figure 8. Verification judgment points in all elements.

6.2. In case core concrete is subject to verification

The seismic performance of the concrete structures targeted by the authors is set so that the structures do not collapse against the standard seismic motion. From the results of section **6.1**, it was found that if the limit value is applied to all the elements of the specimen, it can be evaluated on the very safe side. On the other hand, in order to make an evaluation that reaches the limit state at about the maximum load capacity, it should be applied to the core concrete inside the main reinforcing bar, which is considered to directly affect the load capacity.

Figure 9 shows the load-displacement relationship of each specimen, N-1, P-1, N-2-1, and N-2-2, respectively. Load capacity calculated from the JSCE specifications is also shown in the figure. The position where each index is judged to be in the limit state is indicated by "○". The numbers represent the loading order.

Although $\sqrt{J'_2}$ is still relatively evaluated on the safe side, it was found that the other indices are judged to be in the limit state at about the maximum load capacity.

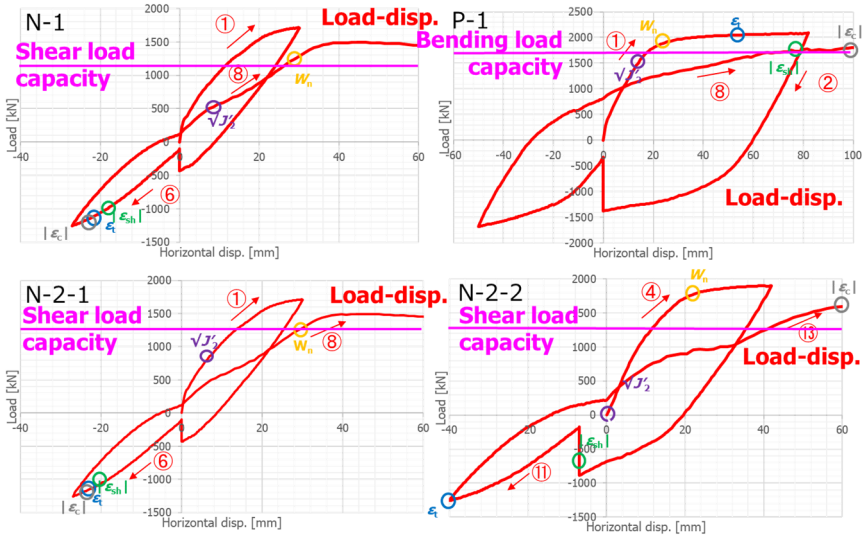

Figure 9. Load-disp. relationships and indicator values.

Figure 10 shows the positions where each index is judged to be in the limit state in each specimen. It can be seen that the index indicating the compressive damage has reached the limit state on the compression side, and the index indicating the tensile damage has reached the limit state on the tensile side. Even if the evaluation area is core concrete, it is possible that the reason why $\sqrt{J'_2}$ is still evaluated on the relatively safe side is that damage due to bending cracks, which is not directly related to load bearing capacity, has an effect. In addition, the principal tensile strain (ε_t), principal compressive strain ($|\varepsilon_c|$), and maximum shear strain ($|\varepsilon_{sh}|$) are element size dependent. However, the evaluation was almost the same as that of an index with a small element size dependence such as W_n. It is presumed that the reason is that if the actual scale RC member is the analysis target, the element size naturally increases and becomes equivalent to the length considered in the averaging region.

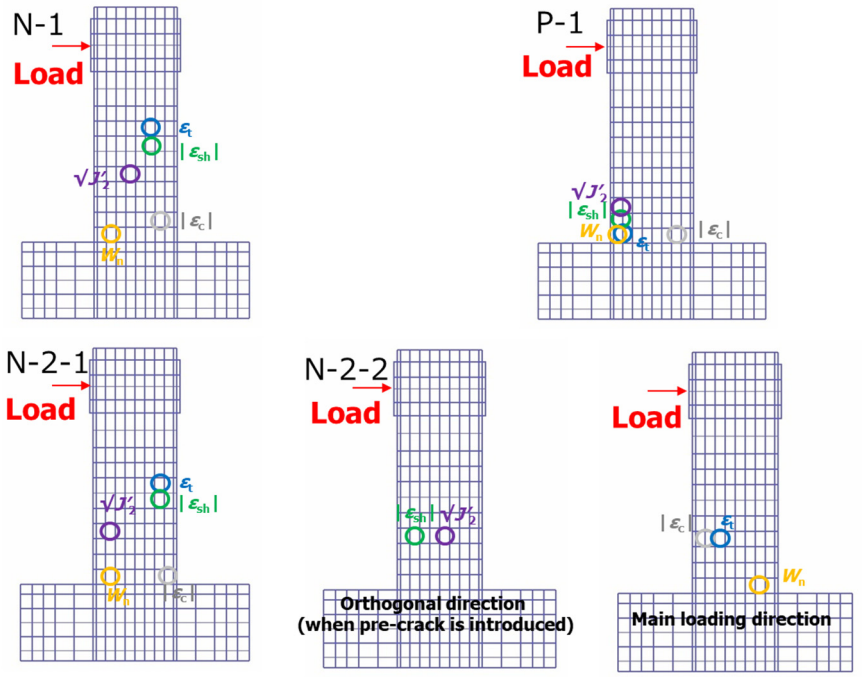

Figure 10. Verification judgment points in core concrete elements.

7. Conclusions

In this paper, the applicability of seismic performance verification indices based on the strain index calculated by three-dimensional material nonlinear FEM analysis to full-scale RC members subjected to horizontal bilateral loadings was verified. As a result, the following conclusions were obtained.

1. It was found that the limit value was reached while maintaining sufficient loading capacity in all the verification indices for all specimens in this study: the specimen with post-installed shear reinforced reinforcements (P-1), the specimen with diagonal tensile failure due to simultaneous force in two horizontal directions (N-2-1), and the specimen with diagonal tensile failure after damage in positive and negative alternation (N-2-2).
2. When all the elements are set as the evaluation area, it is judged that the limit state is reached at the position of the cover concrete, so it was found that the limit state was reached before reaching the maximum loading capacity for all the indices.
3. By using the core concrete as the evaluation area for the verification indices, rational evaluation consistent with the physical phenomenon of a decrease in loading capacity due to the destruction of the core concrete was possible.
4. It was found that $\sqrt{J'_2}$ and W_n were evaluated conservatively compared to other indices.
5. Various strain indices (ε_t, $|\varepsilon_c|$, $|\varepsilon_{sh}|$) that depend on the element dimensions could be evaluated rationally as long as the element dimensions did not change significantly from the average length of 150 mm.

6. Three-dimensional material nonlinear FEM using these indices makes it possible to verify the seismic performance of full-scale RC members subjected to repeated horizontal bilateral loadings leading to shear fracture or bending fracture.

Acknowledgements

This research was carried out as part of the common research of the Nuclear Risk Research Center by nine electric power companies in Japan along with Japan Atomic Power Company, Electric Power Development Co., Ltd., and Japan Nuclear Fuel Limited. In addition, the discussion with Professor Koichi Maekawa from Yokohama National University was helpful. Furthermore, the experiment used for this study was conducted with the cooperation of Taisei Corporation. We gratefully acknowledge all the aforementioned for their cooperation.

References

Nuclear Civil Engineering Committee Japan Society of Civil Engineers (2018). Guideline and Recommendation for Seismic Performance Verification of Underground Reinforced Concrete Structures in Nuclear Power Stations. (in Japanese)

Katsuyuki SAKASHITA, Yujin YAMAMOTO, Akihito HATA, Toyofumi MATSUO and Nobuaki MATSUI. Experimental study on shear capacity of full-scale RC members under two directional loadings. Journal of Structural Engineering, A, Vol. 67A, 2021. (in Japanese)

Seiji NAGATA, Toyofumi MATSUO, Akihito HATA, Yujin YAMAMOTO and Nobuaki MATSUI. Ultimate behavior of full-scale RC members seismically retrofitted by post-installed shear reinforcements based on bilateral loadings tests. The 20th JSMS Symposium on Concrete Structure Scenarios, Vol. 20, pp. 399-404, 2020. (in Japanese)

Satoshi KOMATSU, Seiji NAGATA, Toyofumi MATSUO, Akihito HATA, Koichi Maekawa. Numerical analysis on fracture behavior of full-scale RC member subjected to horizontal bilateral loadings. Journal of Structural Engineering, A, Vol. 67A, 2021. (in Japanese)

Maekawa, K., Pimanmas, A. and Okamura, H. (2003). Nonlinear Mechanics of Reinforced Concrete. Spon Press.

Japan Society of Civil Engineers (2018). Standard Specifications for Concrete Structures-2017 'Design'. (in Japanese)

Shigehiko Saito, Takeshi Maki, Satoshi Tsuchiya and Tadatomo Watanabe. Damage assessment of RC beams by nonlinear finite element analysis. Journal of Japan Society of Civil Engineers, Ser. E2 (Materials and Concrete Structures), Vol. 67, No. 2, pp. 166-180, 2011. (in Japanese)

Takeshi Maki, Satoshi Tsuchiya, Shigehiko Saito and Tadatomo Watanabe. Numerical Evaluation of load-carrying mechanisms of RC columns based on damage of constitutive materials. Journal of Japan Society of Civil Engineers, Ser. E2 (Materials and Concrete Structures), Vol. 71, No. 1, pp. 29-47, 2015. (in Japanese)